Defect equilibria from first principles: From widegap oxides to topological semimetals

Stephan Lany
National Renewable Energy Laboratory, Golden, CO 80401

First International Workshop FLAIR 2024
Fermi Level and Processing of Oxide Electroceramics
March 3-7, 2024

Defect equilibria from first-principles calculations

First-principles supercell calculations

$$\Delta H_{D,q}(\mu, E_F) = [E_{D,q} - E_{host}] + [\mu_{host} - \mu_D] + q \cdot E_F$$

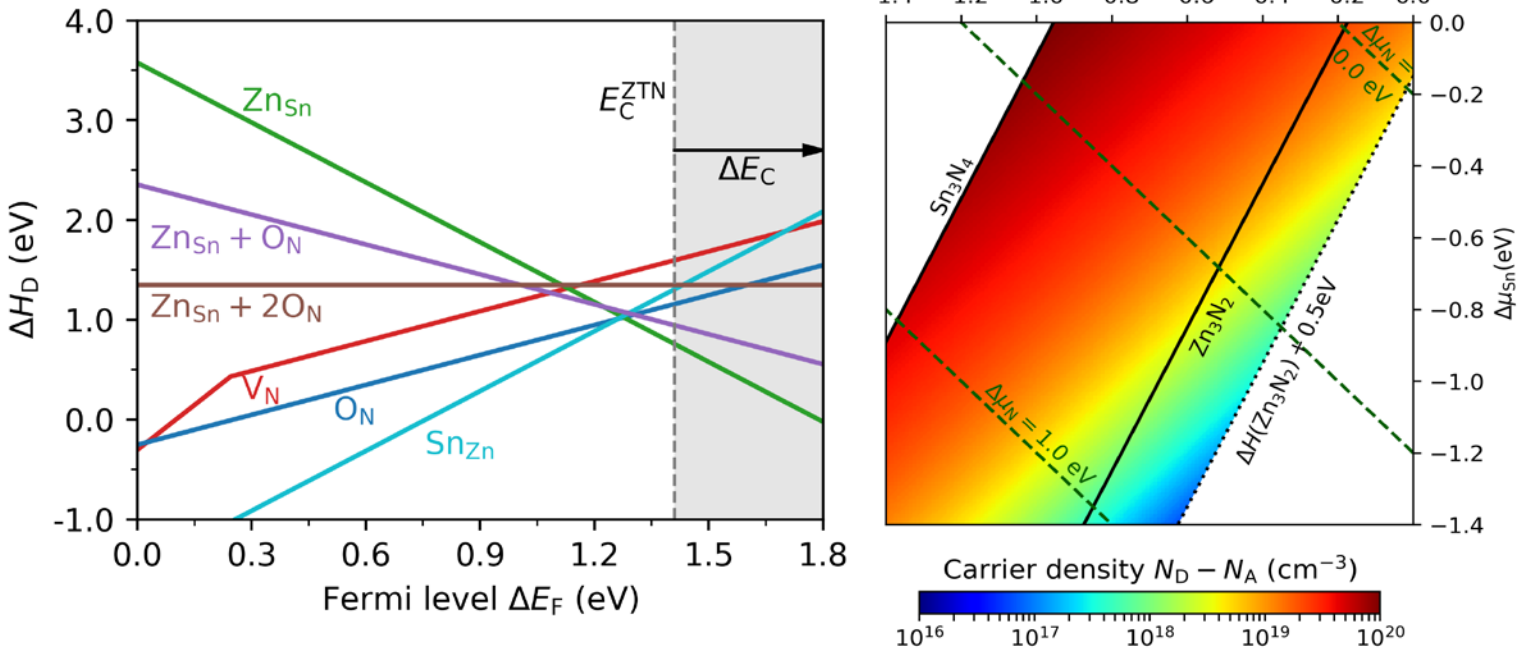

Nonequilibrium Synthesis of $ZnSnN_2$:O
J. Pan, ..., SL, Adv. Mater. 1807406 (2019)

Traditional solid-state chemistry

$$K_{red} = p_{O_2}^{1/2}[V_O^{\bullet\bullet}]n^2$$

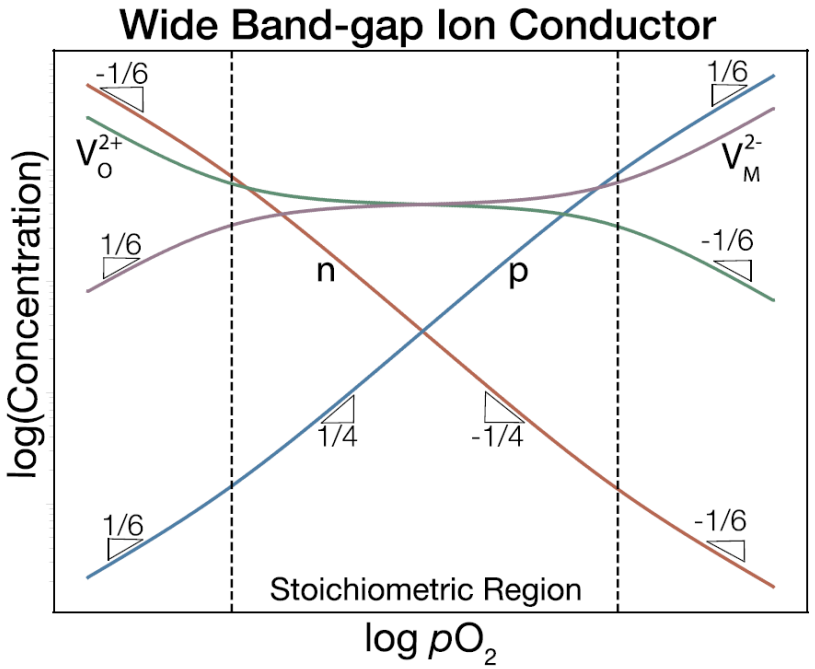

A Convergent Understanding of Charged Defects
S. Anand *et al.*,
Acc. Mater. Res. 3, 685 (2022)

Ideal gas free energy

Gas phase chemical potential

$$\mu_O = \tfrac{1}{2}H(O_2,0K) + \Delta\mu_O(p,T)$$

$$\Delta\mu(p,T) = [H^{\circ *} + c_p(T - T^*)] - T\,[S^{\circ *} + c_p \ln(T/T^*)] + k_B T \ln(p/p^\circ)$$

- standard enthalpy at 1 bar and 298.15K
- heat capacity (3.5 k_B, rigid rotor)
- standard entropy
- pressure dependence (ideal gas law)

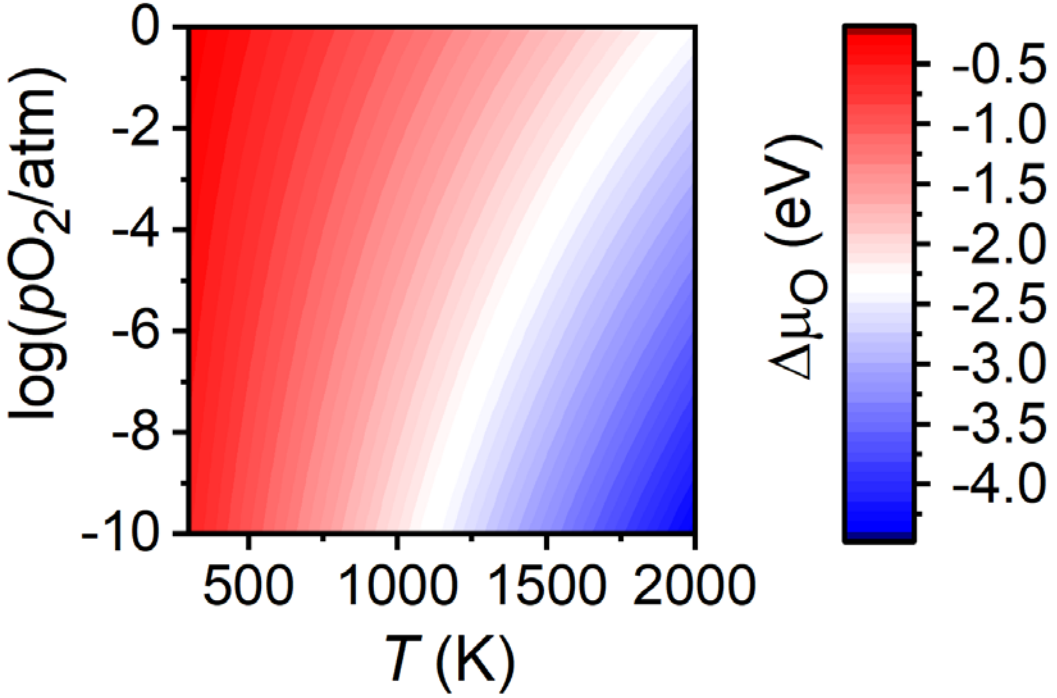

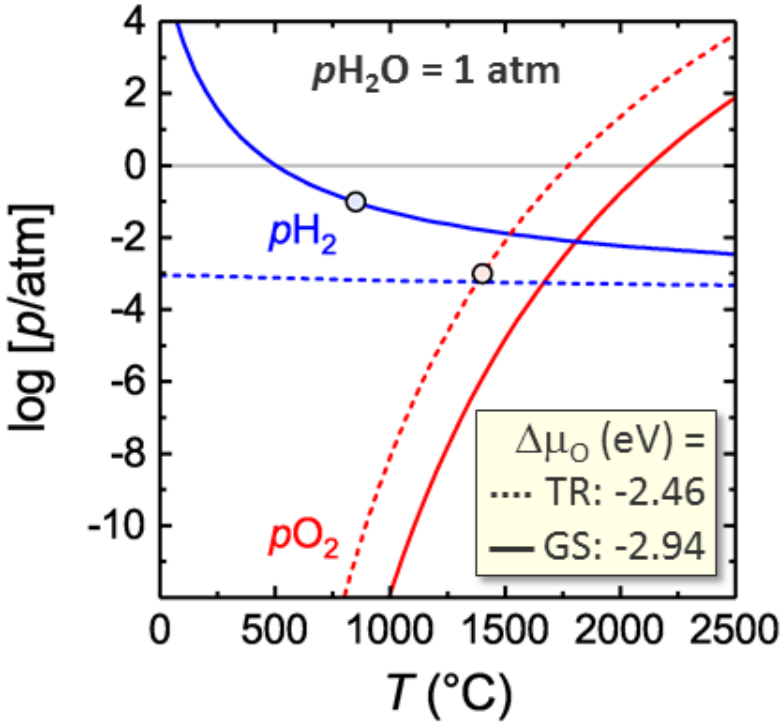

$H_2 + \tfrac{1}{2}O_2 \leftrightarrow H_2O$

SL, J Chem Phys 148, 071101 (2018)

Thermodynamic simulations

Defect formation energy	$\Delta H = \Delta H_{D,q}(\mu, E_F)$
Defect concentration	$c_D \approx N_{site} \times \exp(-\Delta H/kT)$
Electron/hole density	$c_e = \int f_{FD}(E - E_F)\, g(E)\, dE$
Charge neutrality	$-c_e + c_h + \Sigma\,[q \cdot c(D^q)] = 0$
Self-consistent solution	$\Delta H(E_F) \longrightarrow c_D(\Delta H) \longrightarrow E_F$

Association / dissociation of defect pairs and complexes within law of mass action

Direct ($\Delta\mu \rightarrow c_D$) and inverse ($c_D \rightarrow \Delta\mu$) solutions ("pseudo-equilibrium")

Temperature dependence of band gap (CBM and VBM)

SL, JCP 148, 071101 (2018)
Biswas, SL, PRB 80, 115206 (2009)

Outline

(1) Computational Fermi level engineering and doping-type conversion of Mg:Ga_2O_3 via three-step synthesis process

Anuj Goyal, A. Zakutayev, V. Stevanović, S. Lany

J. Appl. Phys. **129**, 245704 (2021)

(2) Band energy dependence of defect formation in the topological semimetal Cd_3As_2

Chase Brooks, M. van Schilfgaarde, D. Pashov, J.N. Nelson, K. Alberi, D.S. Dessau, S. Lany

Physical Review B **107**, 224110 (2023)

(3) Predicting Thermochemical Equilibria with Interacting Defects: $Sr_{1-x}Ce_xMnO_{3-\delta}$ Alloys for Water Splitting

Anuj Goyal, M.D. Sanders, R.P. O'Hayre, S. Lany

PRX Energy **3**, 013008 (2024)

Ga_2O_3 Fermi Level Engineering

Promising properties of β-Ga_2O_3:

- Ultra-wide bandgap (~4.9 eV)
- Tunable *n*-type conductivity
- *p*-type doping?
- Fermi level engineering (w/o *p*-type conduction)

Non-equilibrium doping

- Analogy to GaN:Mg
- Growth under H_2
- Annealing/activation

Nakamura *et al*,
Jpn J Appl Phys 31, 1258 (1992)

Three-step synthesis process

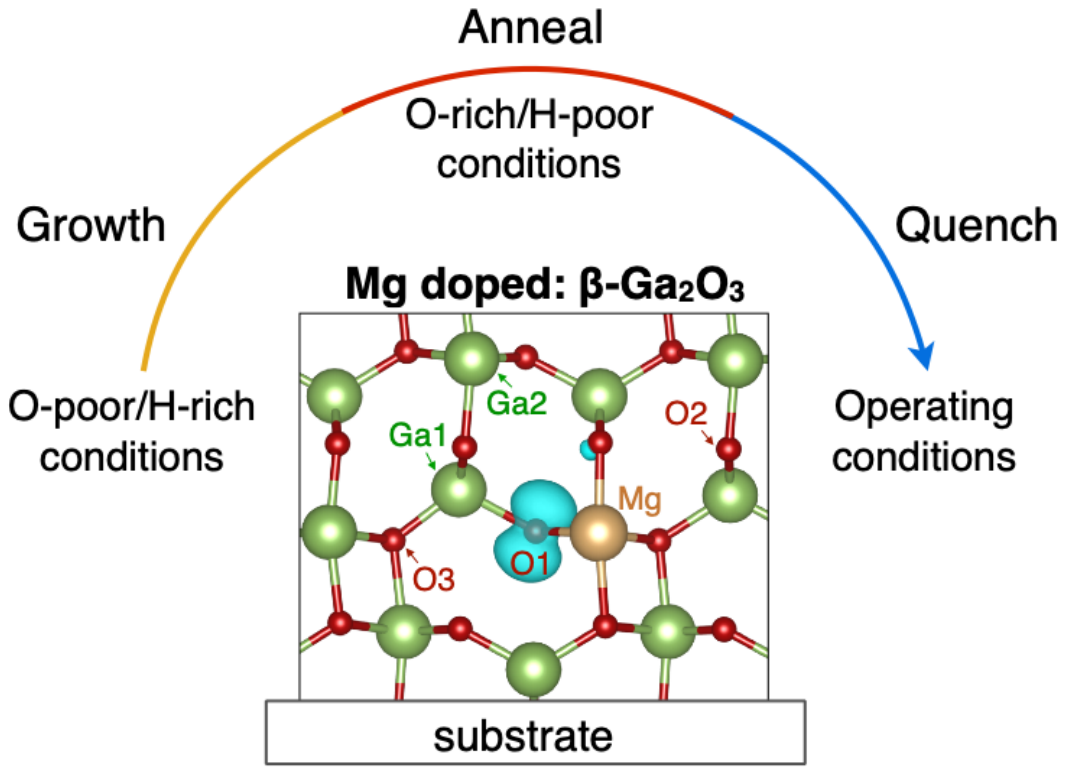

Quantitative computational predictions for process conditions enabling *n*-to-*p* type conversion

Computational approach

DFT supercell calculations

- 160 atom supercells: Mg_{Ga}, Mg_i, V_O, V_{Ga}, H_i
- Defect pairs/complexes: ($2Mg_{Ga}$ - V_O), (Mg_{Ga} - H_i)
- VASP-PAW in DFT-GGA (HSE06 for Mg_{Ga} acceptor)
- Fitted elemental reference energies (FERE)
  SL, PRB (2008); Stevanovic *et al*, PRB (2012)
- GW band gap and ΔH_D corrections
  Peng *et al*, PRB (2013)
- *T*-dependence of CBM
  SL, APL Mater (2018)

First principles defect equilibria

- Finite-temperature free energies
  - configurational: defects, pairs, complexes
  - electronic: Fermi-Dirac E_F, CBM(*T*)
  - ideal gas: O_2, H_2, H_2O
  - vibrational: minor contribution
    Millican, ..., SL, Chem Mater (2022)

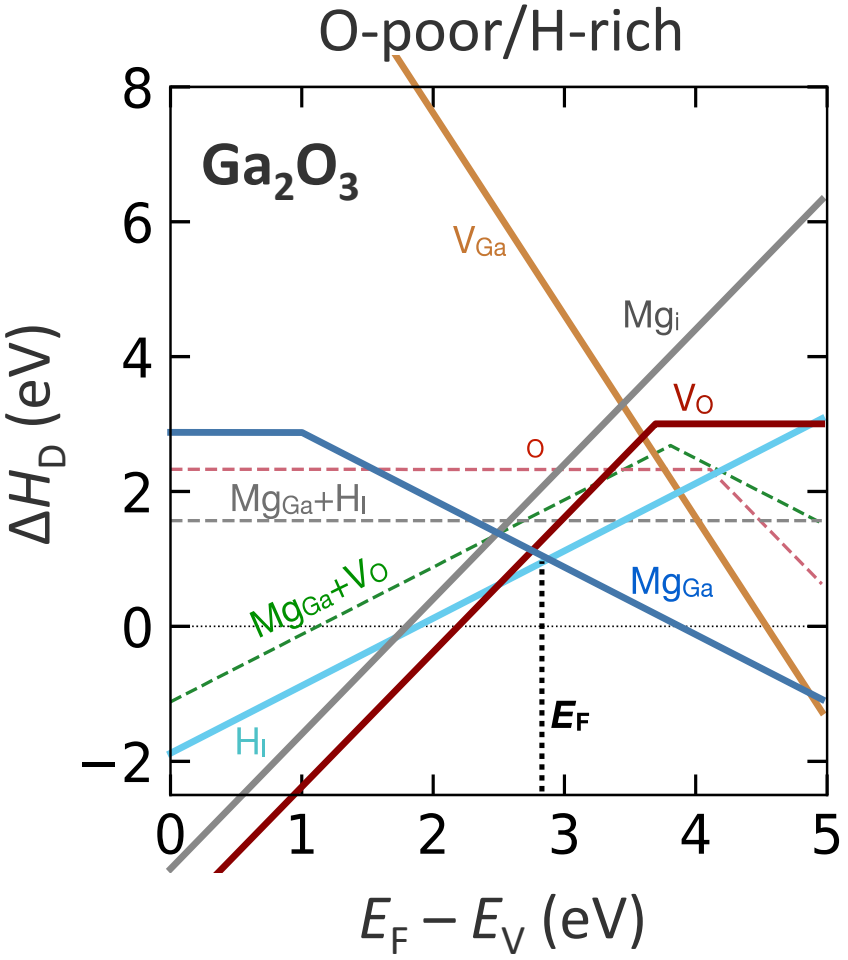

Mg:Ga_2O_3 Growth Step

Mg solubility

$pH_2O = 10^{-5}$ atm

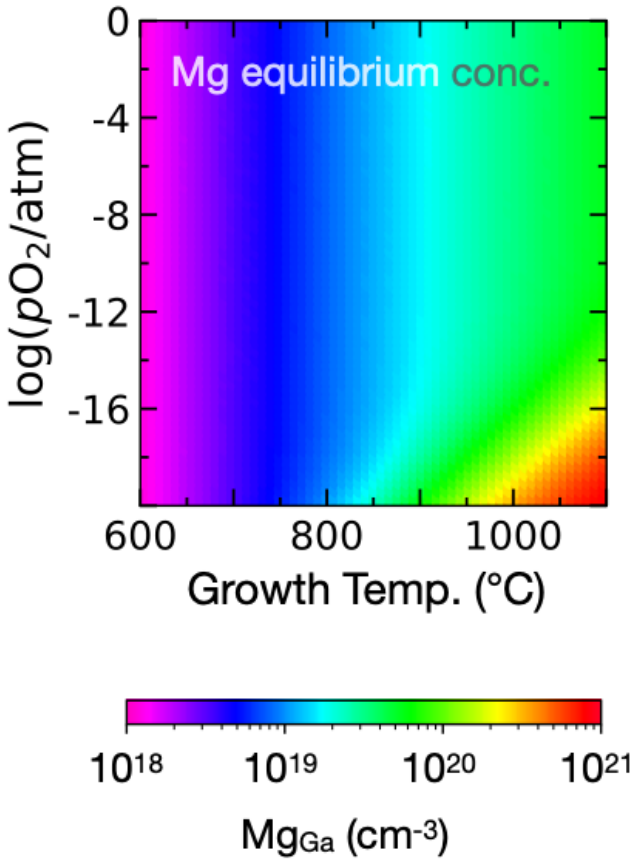

N_a^{pre} vs (Mg,pH_2O)

T = 600 °C, $pO_2 = 10^{-9}$ atm

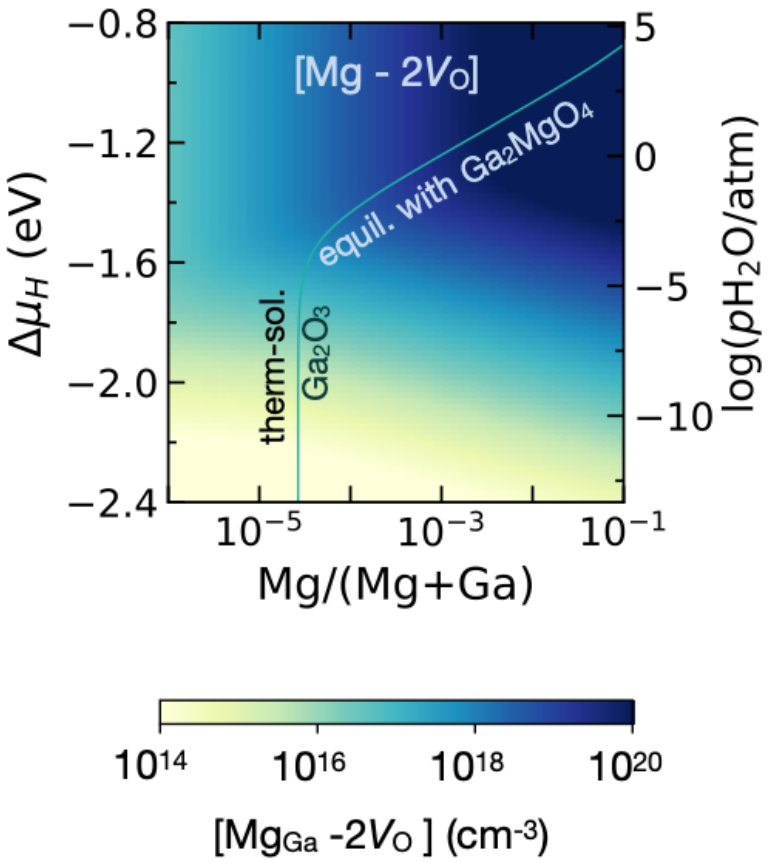

N_a^{pre} vs (T,pO_2)

$pH_2O = 10^{-5}$ atm, Mg = 1%

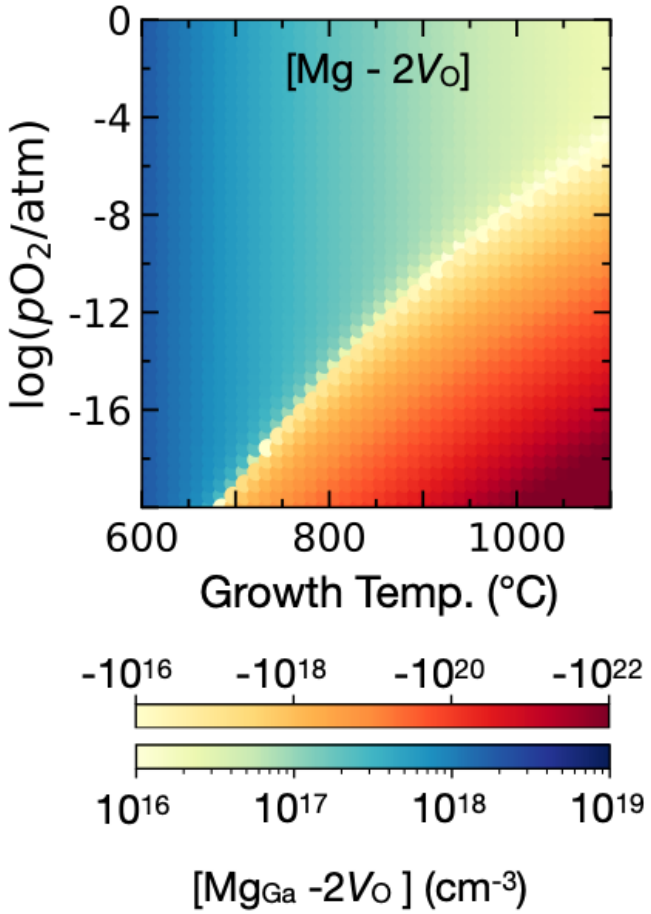

Lower growth T and H-rich conditions required to maximize [Mg – $2V_O$] defect concentration

Annealing Step: Maximize Net Acceptor Concentration

Anneal with V_O equilibration

pO_2 = 1 atm, pH_2O = 10^{-8} atm

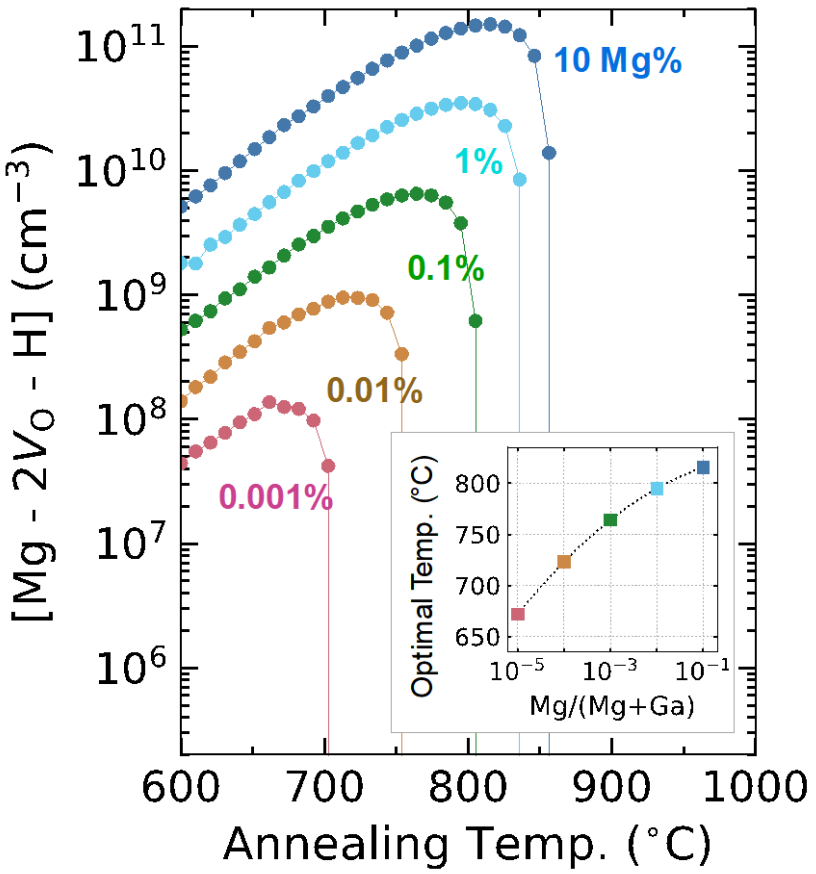

Optimal annealing temperature

Anneal without V_O equilibration

T = 600 °C, pO_2 = 1 atm, pH_2O = 10^{-8} atm

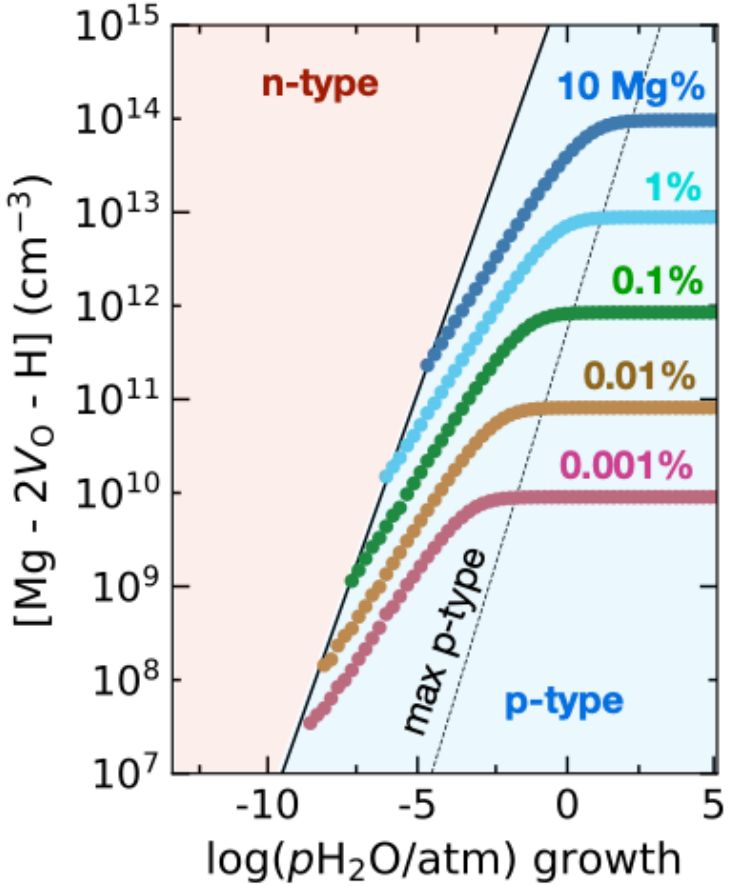

Minimum H (H_2O) required for type conversion

Quench Step: Determine Fermi Level at Operating Conditions

- Quenched from the preceding anneal step
- Freeze defect concentrations and allow for Fermi level (*e*,*h*) to equilibrate

Quench from equilibrium anneal

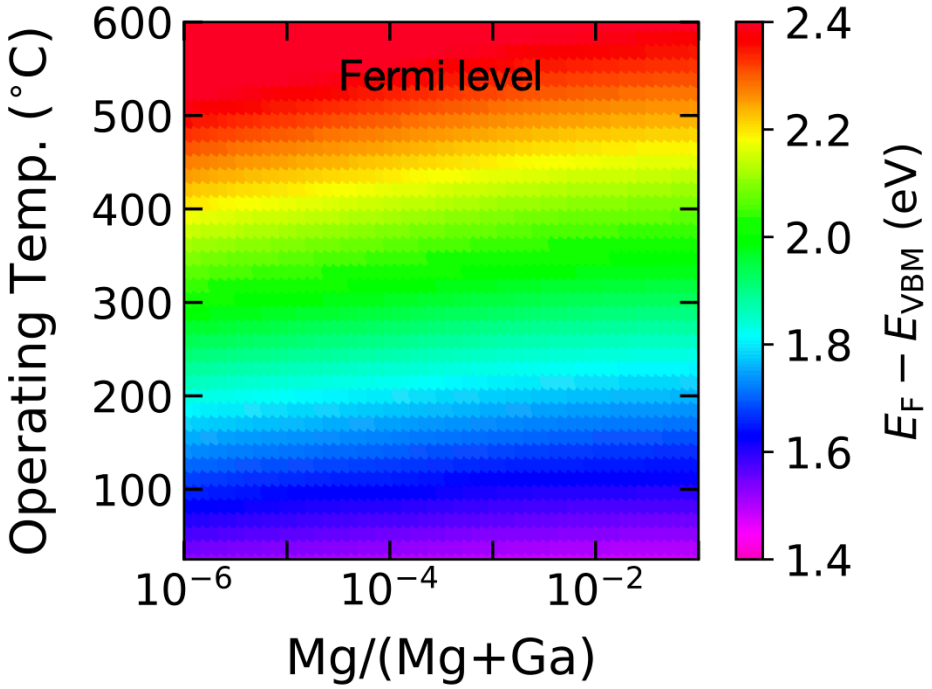

Quench from non-equilibrium anneal

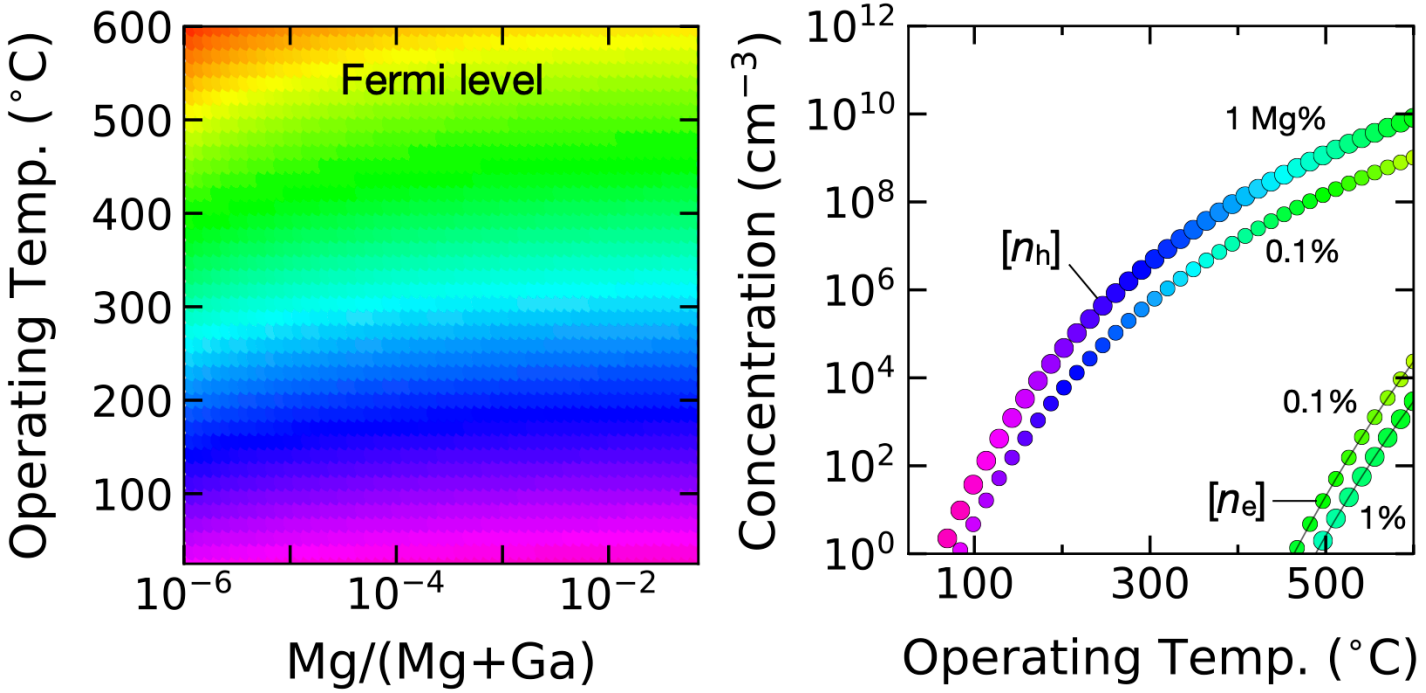

E_F has stronger dependence on T_{op} than Mg doping
$[n_e]$ greatly suppressed

E_F engineering of Ga_2O_3: Conclusions

Defect equilibria from first principles

- Increasing complexity
  - dopant-defect pair association
  - non-equilibrium processes
  - *T* dependence of electronic structure
  - gas phase equilibria
    $H_2 + ½O_2 \leftrightarrow H_2O$

A. Goyal, *et al.*
J Appl Phys 129, 245704 (2021)

Growth

- Little effect of H on Mg solubility
- Reduction of V_O compensation (H-rich and low *T*)

Annealing

- With V_O equilibration: Optimal annealing *T*
- Without V_O equilibration: dependence on growth step

Quench

- Net *p*-type 10^{10} to 10^{13} cm^{-3}
- Negligible *p*-type conductivity
- Reduction of E_F, suppression of n_e

Band Energy Dependence of Defect Formation Topological Semimetal Cd_3As_2

"Disorder in Topological Semimetals" (DOE-SC-BES)

NREL
Kirstin Alberi
Mark van Schilfgaarde

CU Boulder
Chase Brooks
Dan Dessau

- Fermi level within band continuum
- Meaning of defect levels
- Electronic screening
- Shape of the density of states
- Temperature dependence of defect equilibrium
- Doping engineering:
  Avoid unintentional *n*-type doping

Cd_3As_2 structure

Fluorite structure (sg 225)

$CaF_2 \leftrightarrow AsCd_2$

Conventional cell: 12 atom (sc)

Primitive cell: 3 atom (fcc)

2 empty sites per sc cell
for Cd_3As_2 stoichiometry

ground state
sg 142, centrosymmetric
no spin splitting
80 atom primitive cell

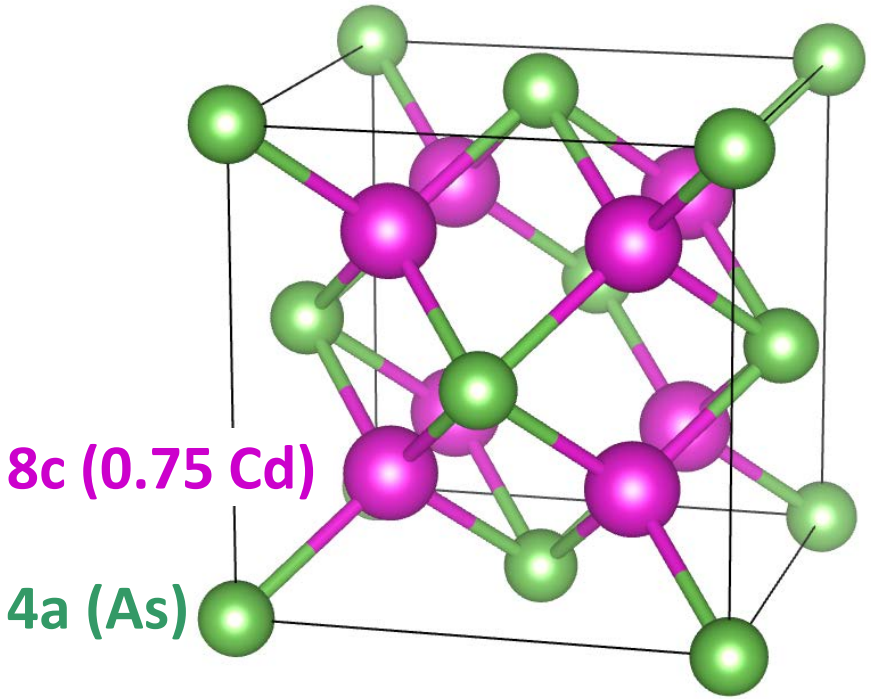

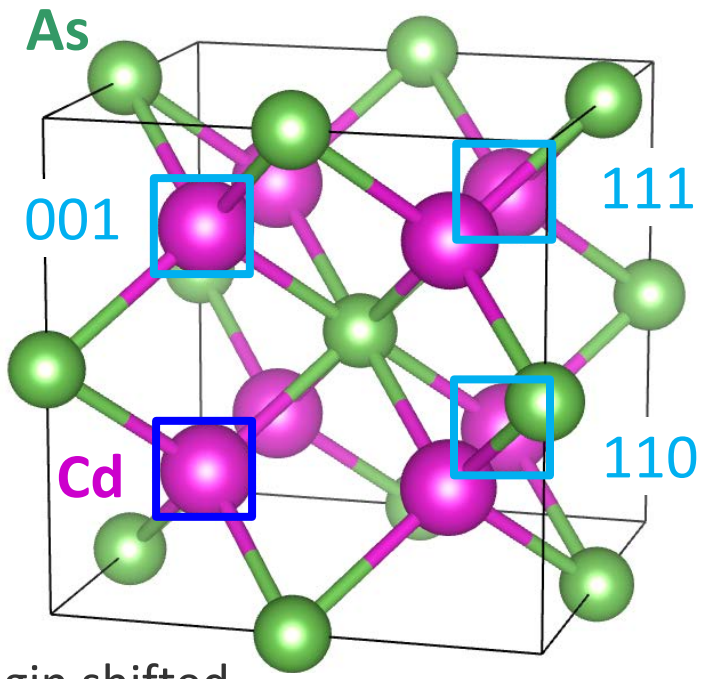

origin shifted
by (0.5, 0.5, 0.5)

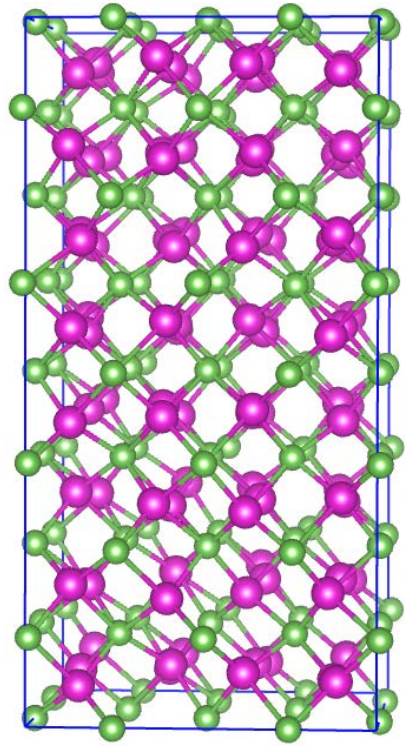

Ali *et al*, Inorg Chem 53, 4062 (2014)

Supercell and electronic structure calculations

First principles calculations

- DFT-PBE (VASP)
- DFT-SCAN + spin-orbit (VASP)
- QSGW electronic structure (Questaal)

Defect formation energy

- Cd interstitial on empty site
- Charged vs neutral defect
- Cell size dependence 80 to 320 atoms

$$\Delta H_{\mathrm{D},q}(E_{\mathrm{F}},\{\mu\}) = [E_{\mathrm{D},q} - E_{\mathrm{h}}] + \sum_{\alpha} n_{\alpha}\mu_{\alpha} + qE_{\mathrm{F}}$$

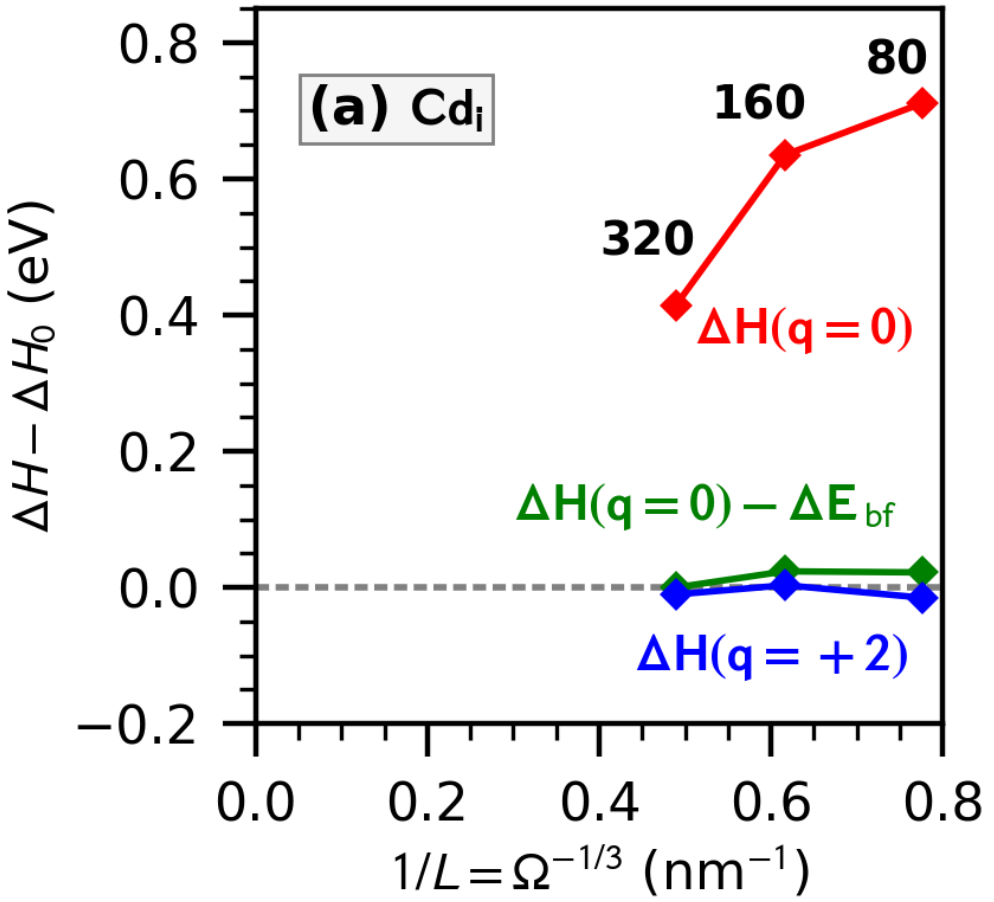

DOS

Defect behavior

- Localized Defect (LD) state vs band continuum (BC)
- Cd_i donors (BC)
- V_{Cd} acceptor (BC)
- V_{As} amphoteric (LD)
- no bound effective-mass donor/acceptor state due to screening

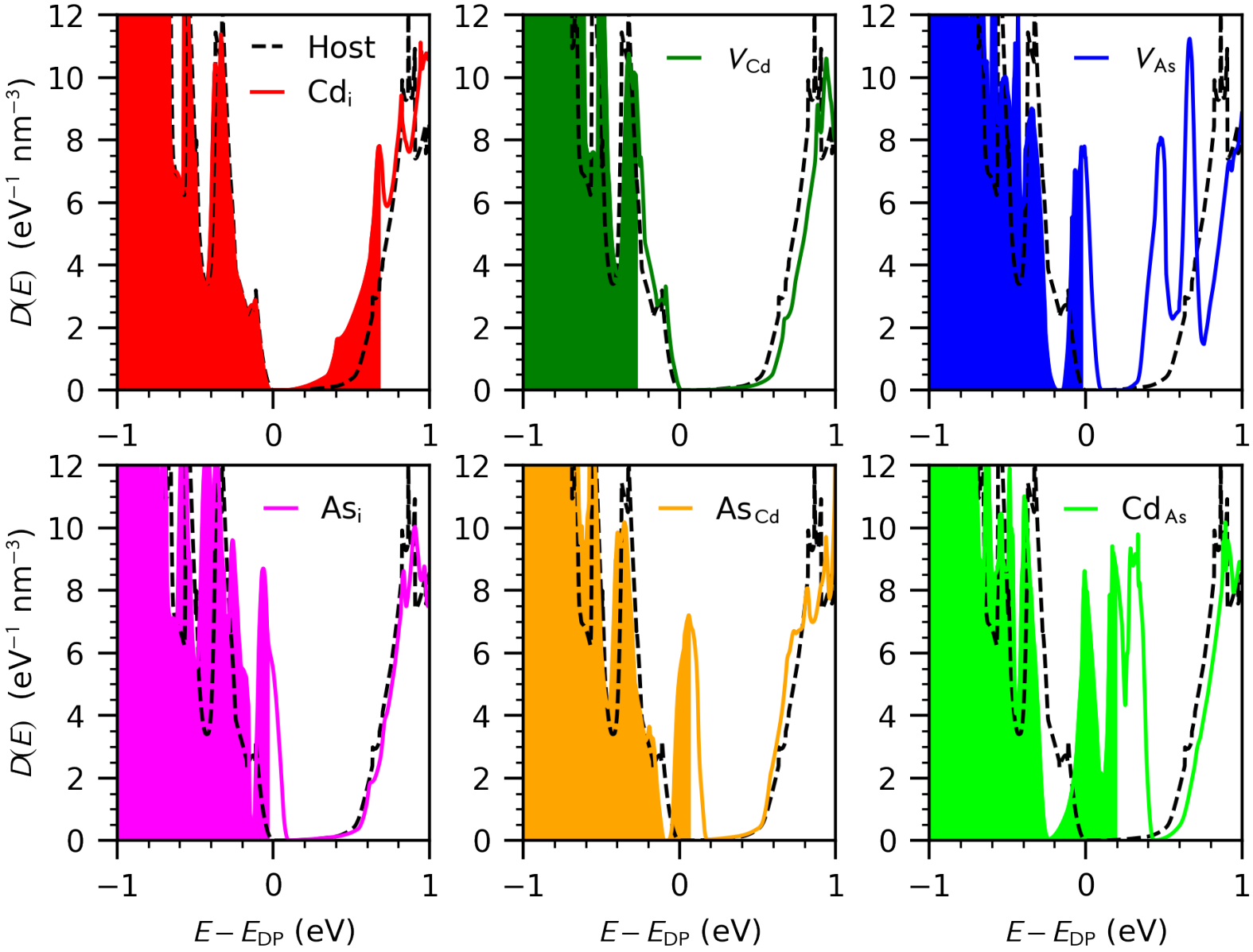

Origin of cell size dependence of ΔH_D

$$\Delta E_{\mathrm{bf}} = \sum_{\substack{n,\mathbf{k} \\ \varepsilon_{n,\mathbf{k}} > E_{\mathrm{DP}}}} w_{\mathbf{k}} f_{n,\mathbf{k}} (\varepsilon_{n,\mathbf{k}} - E_{\mathrm{DP}})$$

Band filling energies

- Dopant donates electrons
- Concentration dependence
- BF energy recovers $\Delta H_D(Cd_i^{2+})$
- Cd_i^0 better described as Cd_i^{2+} + 2e

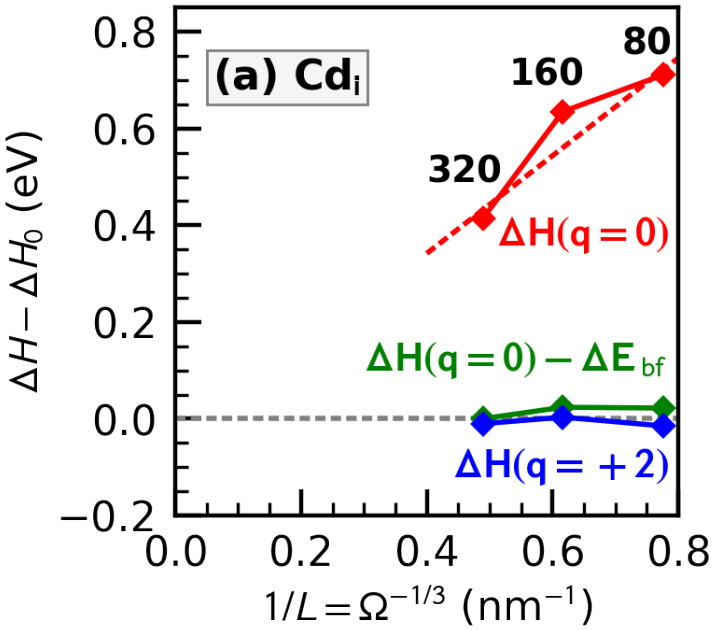

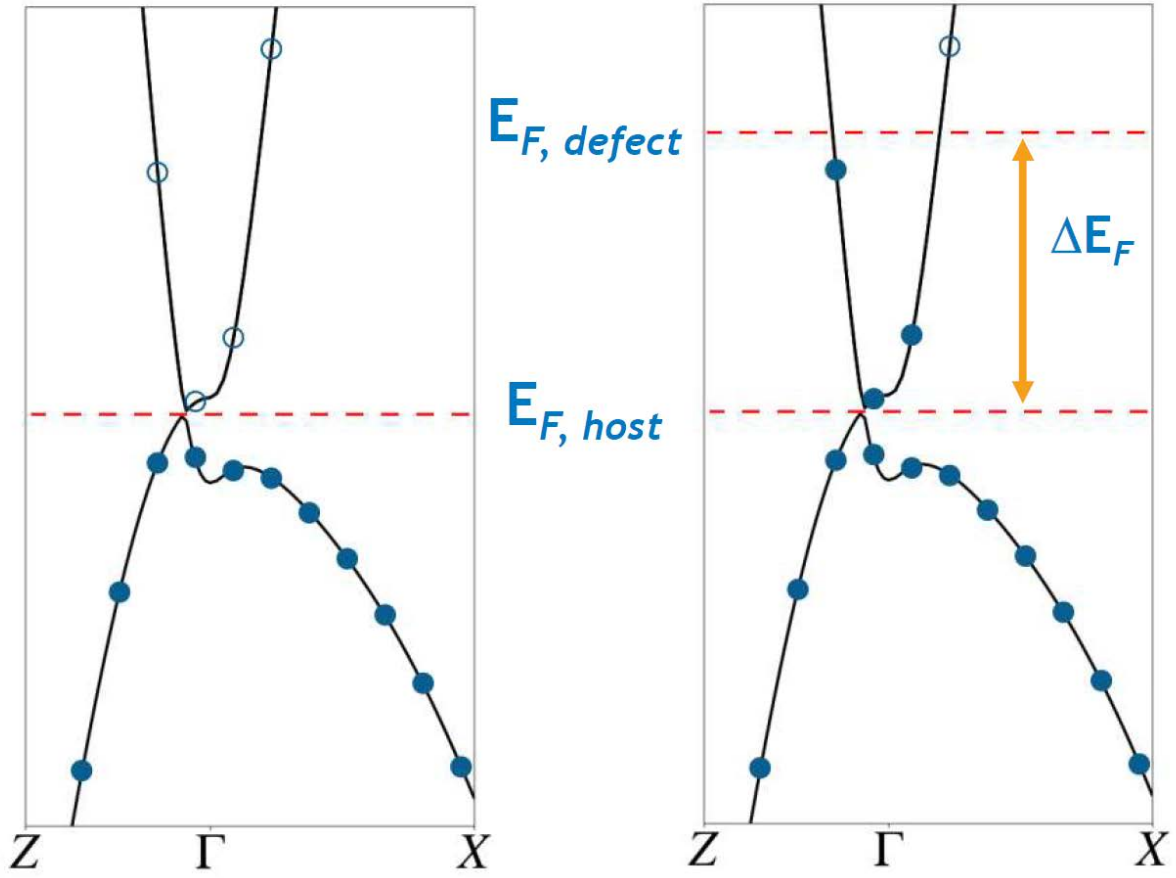

$$\Delta H_{\mathrm{D},q}(E_{\mathrm{F}}, \{\mu\}) = [E_{\mathrm{D},q} - E_{\mathrm{h}}] + \sum_{\alpha} n_\alpha \mu_\alpha + q E_{\mathrm{F}}$$

Electronic structure

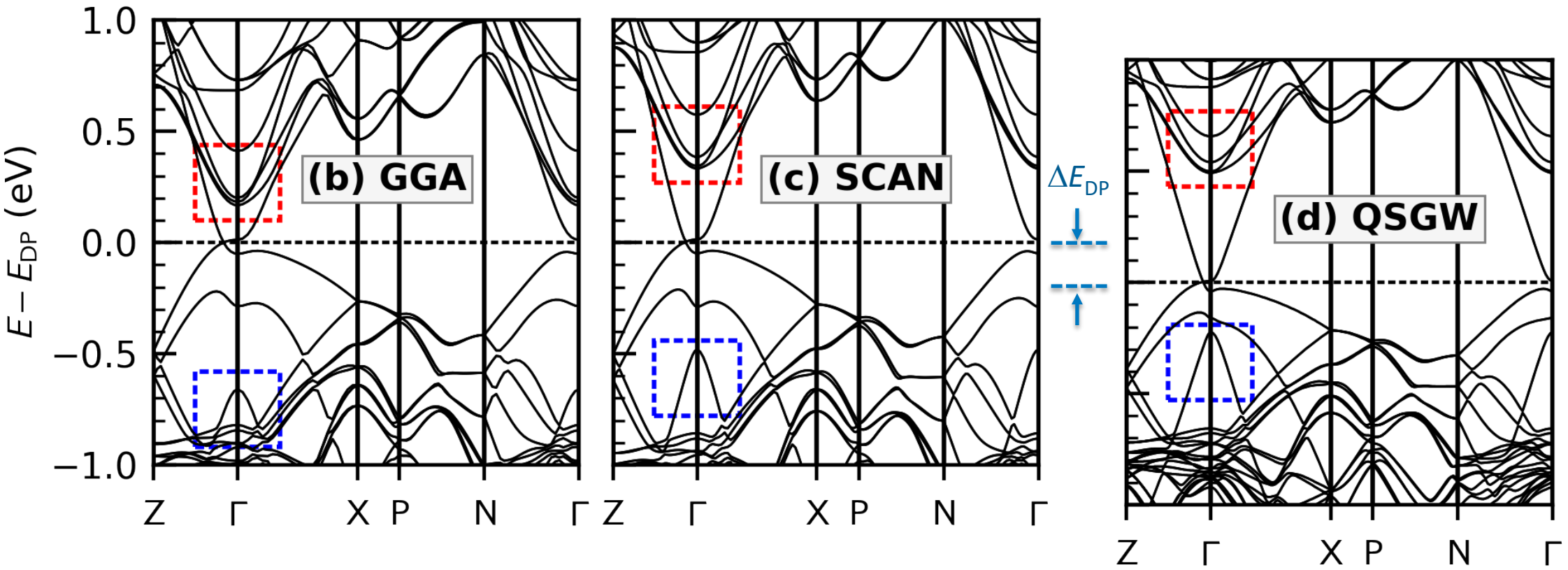

- SCAN lies halfway between standard DFT (GGA) and QSGW
- Upward shift of *s*-like Cd and As states, analogous to semiconductors
- Offset ΔE_{DP} –0.19 eV on absolute energy scale

Defect equilibria

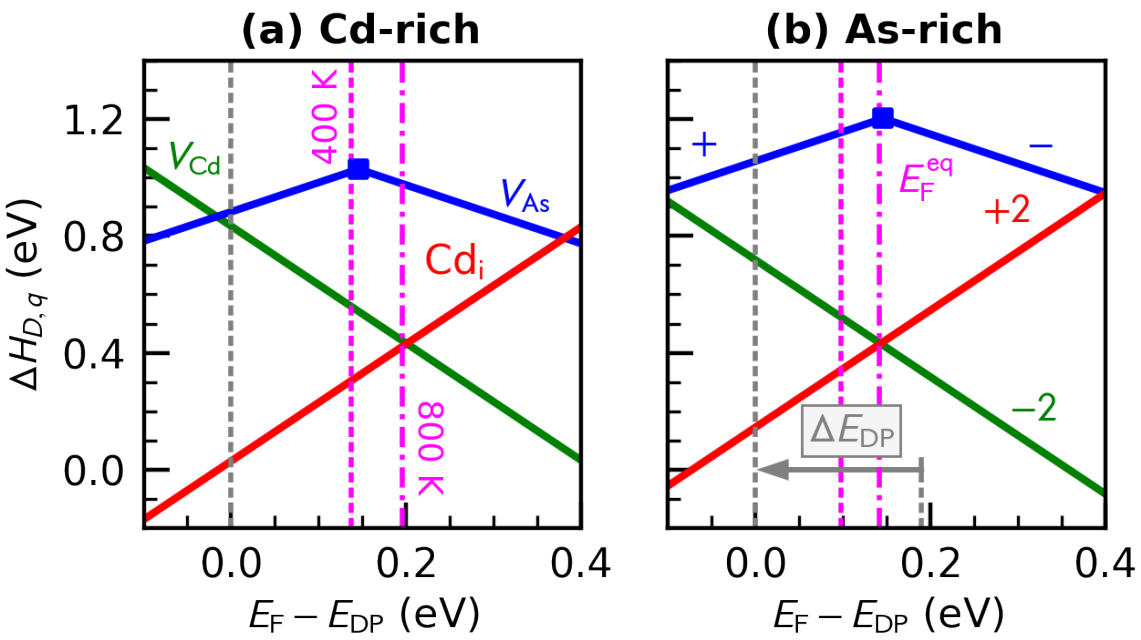

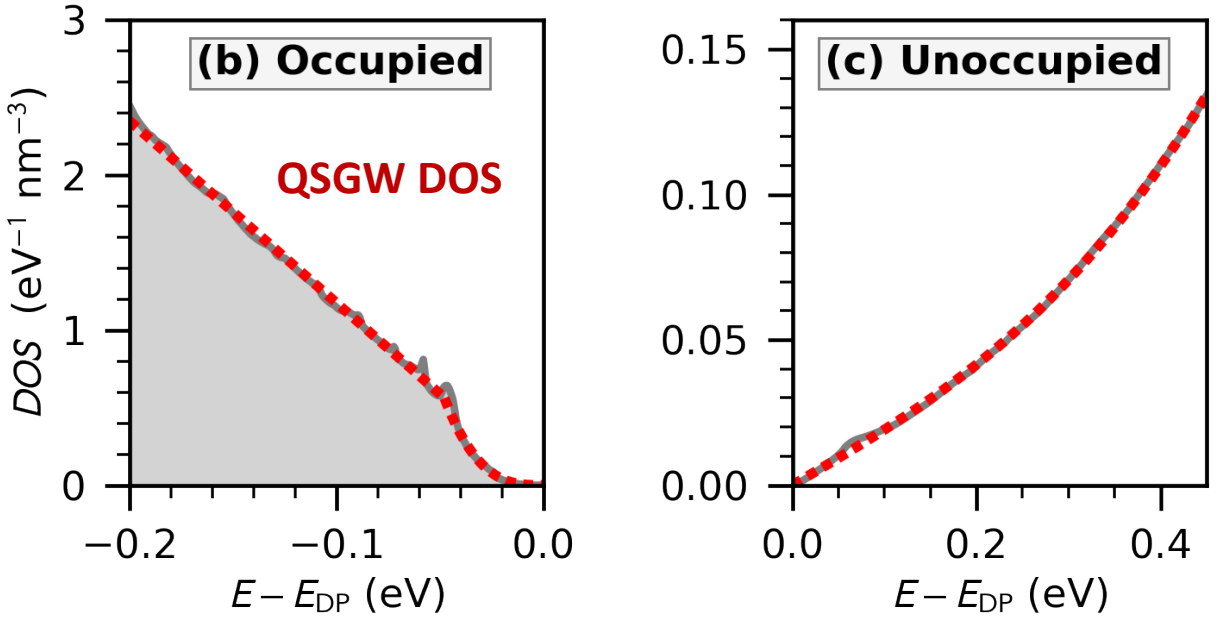

- Cd_i and V_{Cd} are dominant defects, difference determines doping
- Defect equilibrium with charge balance (defects and carriers)

$$n_e = \int_{E_{DP}}^{\infty} \frac{g_{QSGW}(E)}{e^{(E-E_F)/k_B T} + 1} dE$$

Doping-balance control via T_{growth}

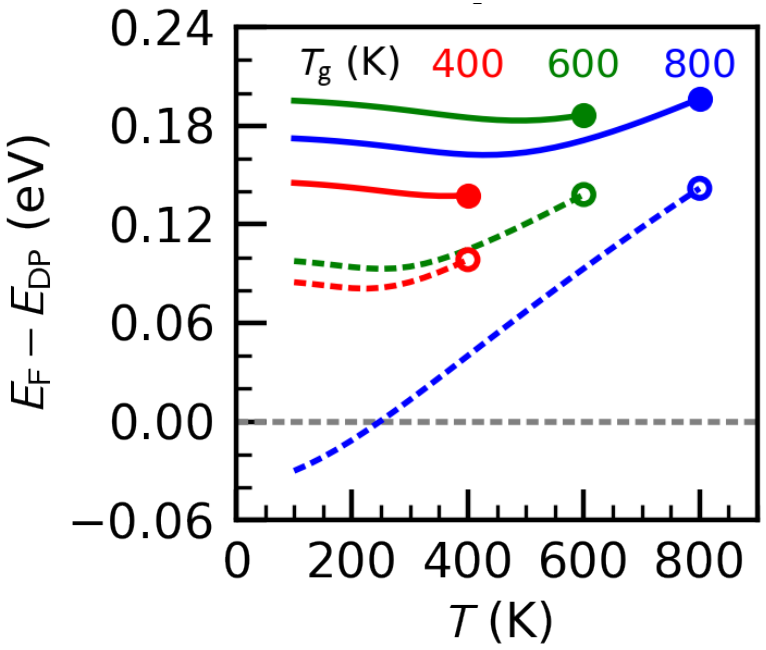

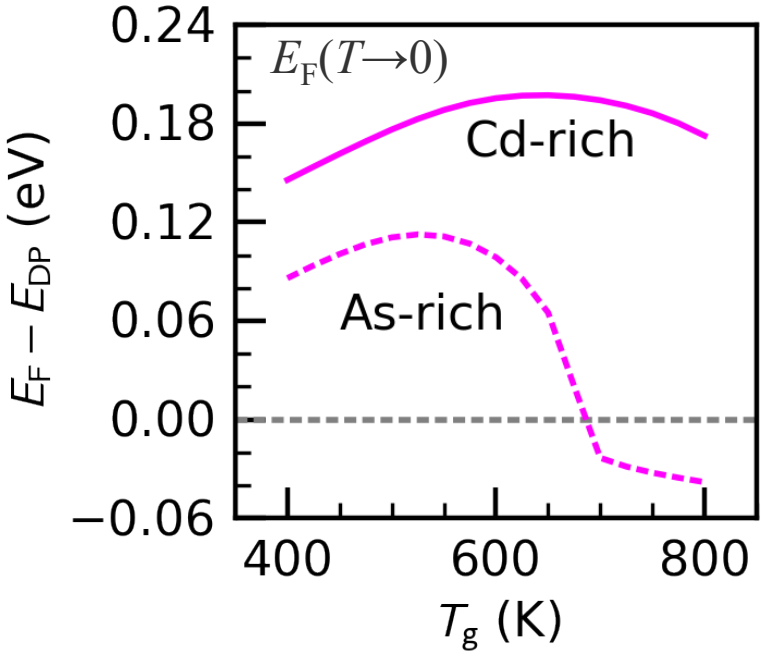

Equilibrium E_F increases with

- Cd-rich (Cd) vs As-rich ($CdAs_2$)
- growth temperature

Constrained equilibrium

- fixed defect conc.
- re-equilibrate $E_F(T)$
- $E_F(T)$ intersects E_{DP} for As-rich/high-T growth

Doping balance control

- non-monotonic behavior
- type conversion

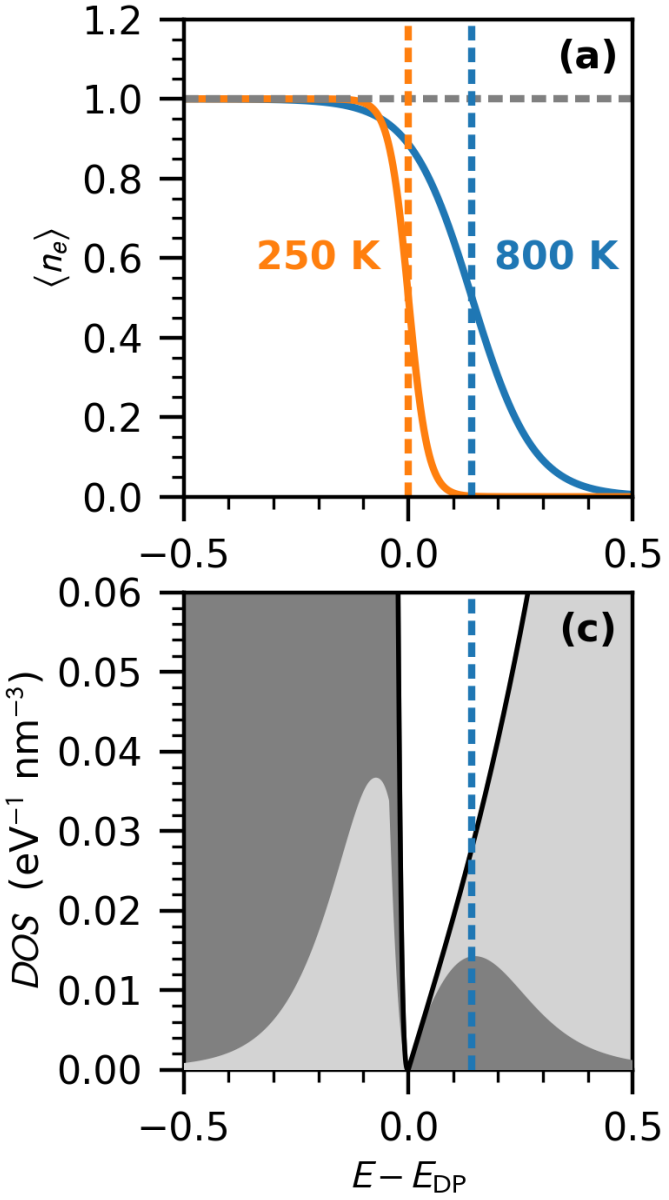

Cd_3As_2 topological semimetal: Conclusions

Defect theory in semimetals

- Absence of bound effective-mass states
- Charged defect + continuum carriers dopants model
- Defect equilibrium and E_F sensitive to shape of DOS

Doping control

- Non-monotonic *T*-dependence of net doping
- Doping balance at specific growth conditions

C. Brooks *et al.*,
Phys Rev B **107**, 224110 (2023)

Solar fuels: Thermochemical Hydrogen

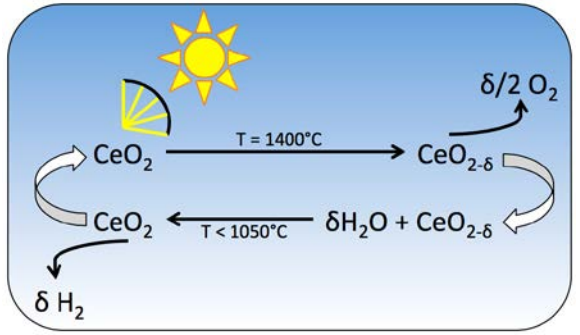

Renewable energy-form mismatch

Renewable Energy additions[1]
(actual power, not capacity)

- Photovoltaics 40%
- Wind 35%
- Hydro 20%

Energy consumption[2]

- Electricity 20%
- Fuels 80%

[1] Renewable capacity statistics IRENA (2023)

[2] Key World Energy Statistics IEA (2021)

$$M_xO \rightarrow M_xO_{1-\delta} + \frac{\delta}{2} \cdot O_2$$

Reduction (solar heat)

$$M_xO_{1-\delta} + \delta \cdot H_2O \rightarrow M_xO + \delta \cdot H_2$$

Oxidation (H_2 production)

$$H_2 + \tfrac{1}{2}\, O_2 \leftrightarrow H_2O$$

Ideal gas law (H_2, O_2, H_2O)

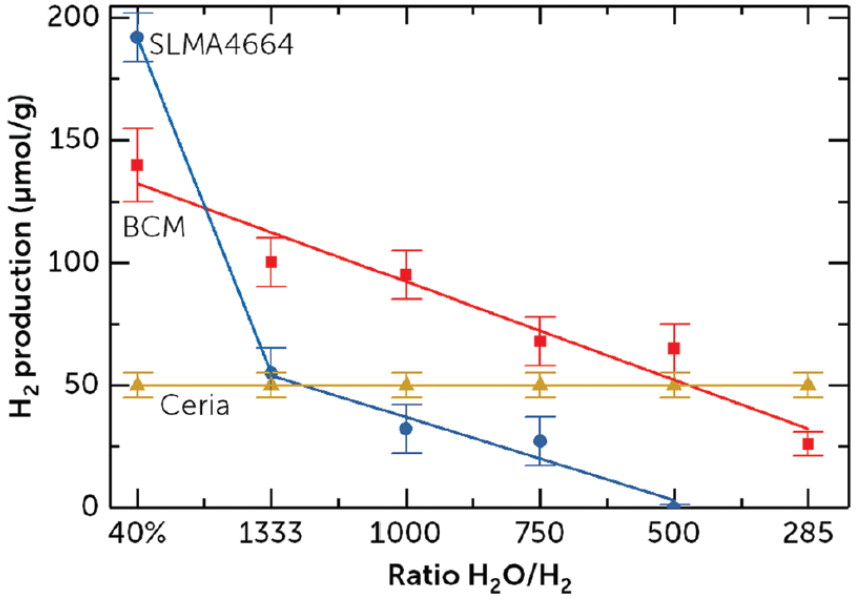

Colorado School of Mines
(R. O'Hayre)

- BCM: $Ba(Ce_{0.25}Mn_{0.75})O_3$
  D. Barcellos *et al.*, EES (2018)
- SCM: $(Sr,Ce)MnO_3$
  A.M. Bergeson-Keller *et al.*, Energy Tech. (2022)

Machine leaning of defects

Model: HT-DFT + dGNN

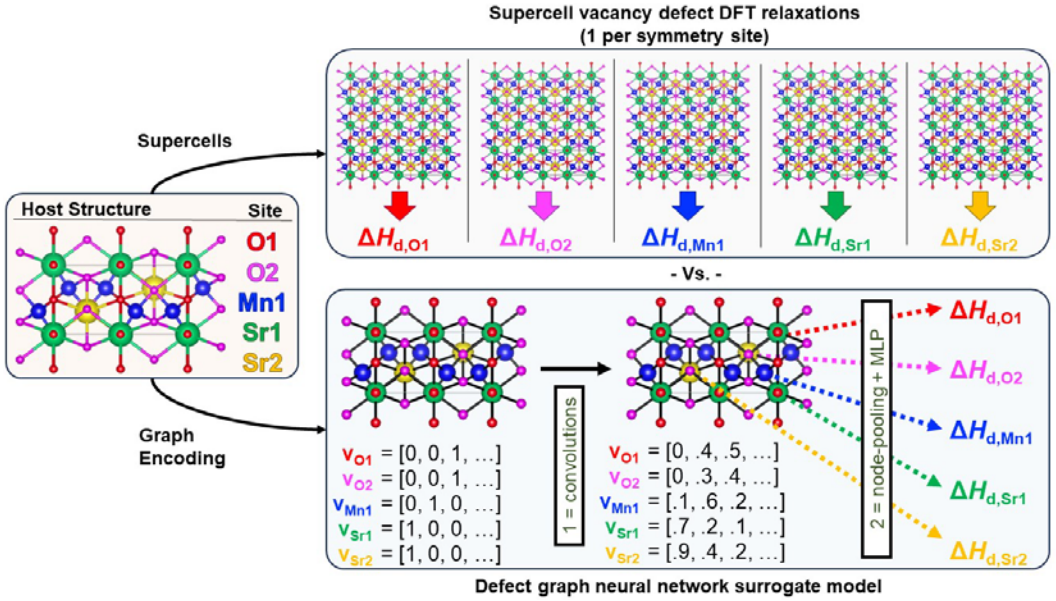

cross-validation

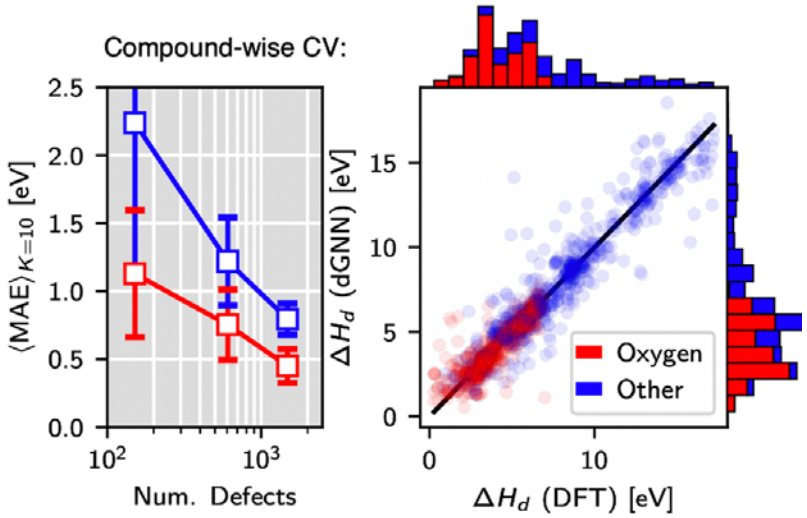

database screening

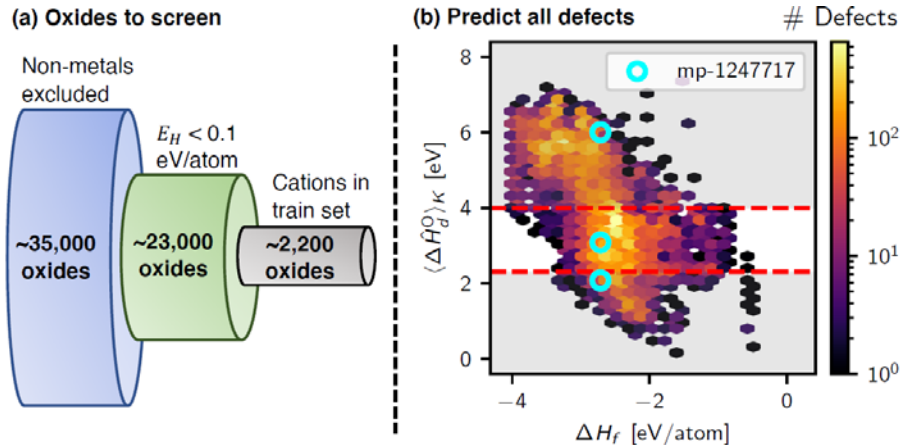

HT-thermodynamics

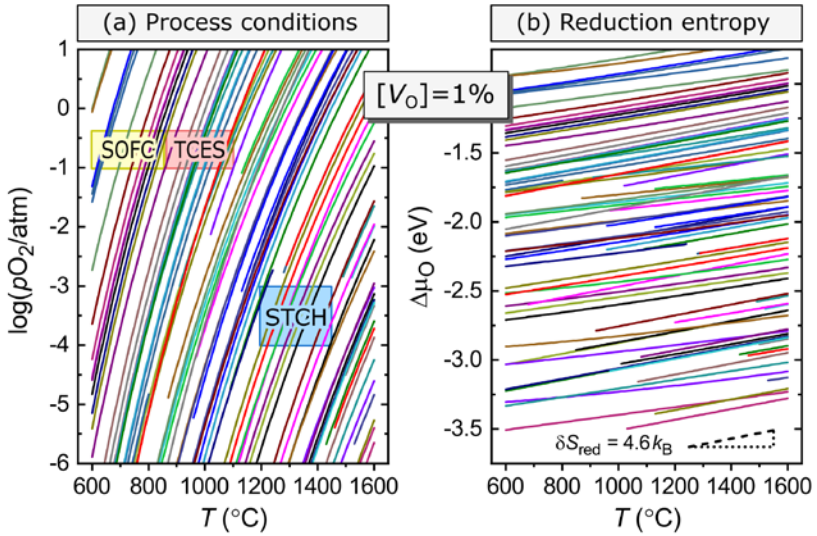

M.D. Witman, A. Goyal, T. Ogitsu, A.H. McDaniel, S. Lany, Nature Comp. Sci. **3**, 675 (2023).

HydroGEN
Advanced Water Splitting Materials

O vacancy formation in $SrMnO_{3-\delta}$

Energy Materials Network (DOE-EERE)

Supercell calculations

- VASP-SCAN+U
  $U_{Mn\text{-}d}$ = 2 eV
  $U_{Ce\text{-}f}$ = 1 eV

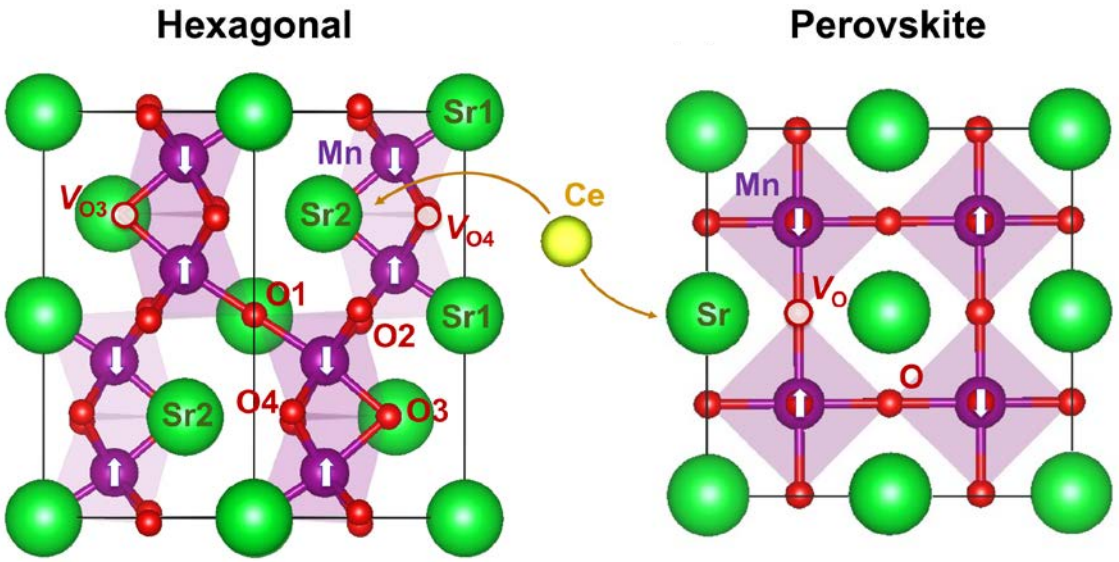

hex	$d_{Mn\text{-}O}$ (Å)	Mn-O-Mn (°)	ΔH_D^{ref} (eV)
O1/O2	1.89-1.92	82	2.37
O3/O4	1.87-1.89	171-174	3.30
perov			
O1	1.90	180	2.04

Role of repulsive defect interactions?

δ = 1.7 @ 1400 °C

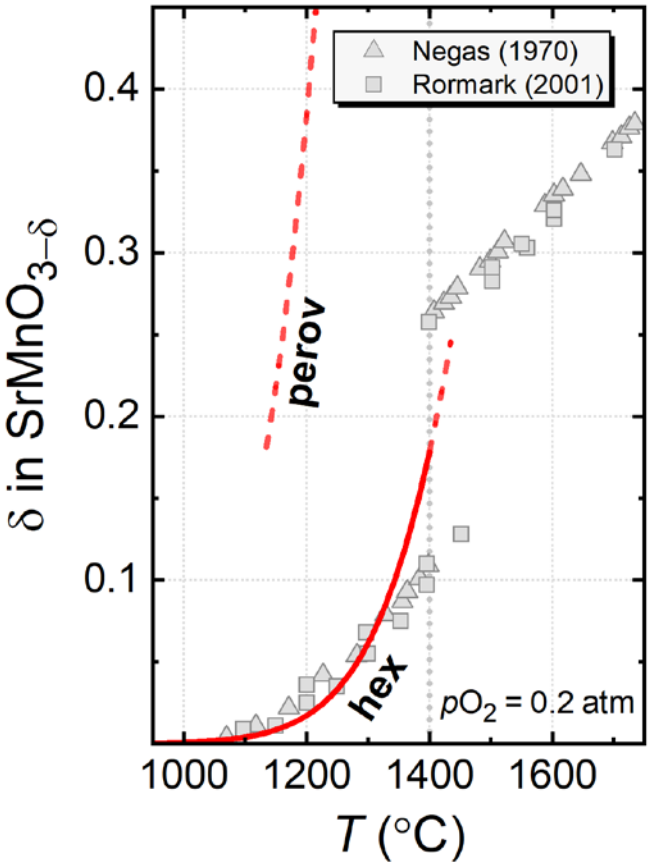

$$\Delta H_D = \Delta H_D^{ref} + \Delta\mu_O$$

$$[V_O] = \frac{\exp(-\Delta H_D / k_B T)}{1 + \exp(-\Delta H_D / k_B T)}$$

Defect model

Free energy of defect interaction

$$\Delta E_i^{\text{int}} = \Delta H_{\text{D},i}(nV_{\text{O}}) - n \times \Delta H_{\text{D}}(V_{\text{O}})$$

$$\Delta G^{\text{int}} = -\frac{k_{\text{B}}T}{n} \ln \sum_i \left(g_i \exp\left(-\Delta E_i^{\text{int}} / k_{\text{B}}T \right) \right)$$

$$\Delta G^{\text{int}}(T) = (a_0 + a_1 T)\delta$$ parameterization

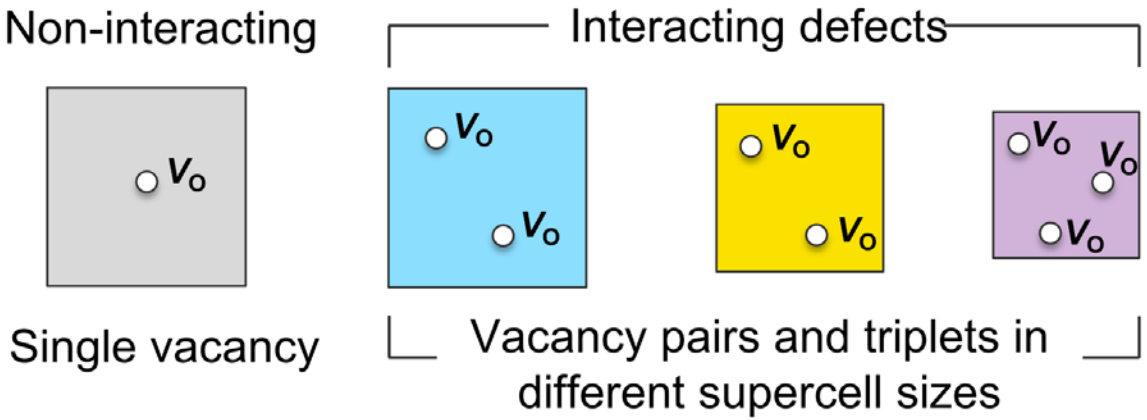

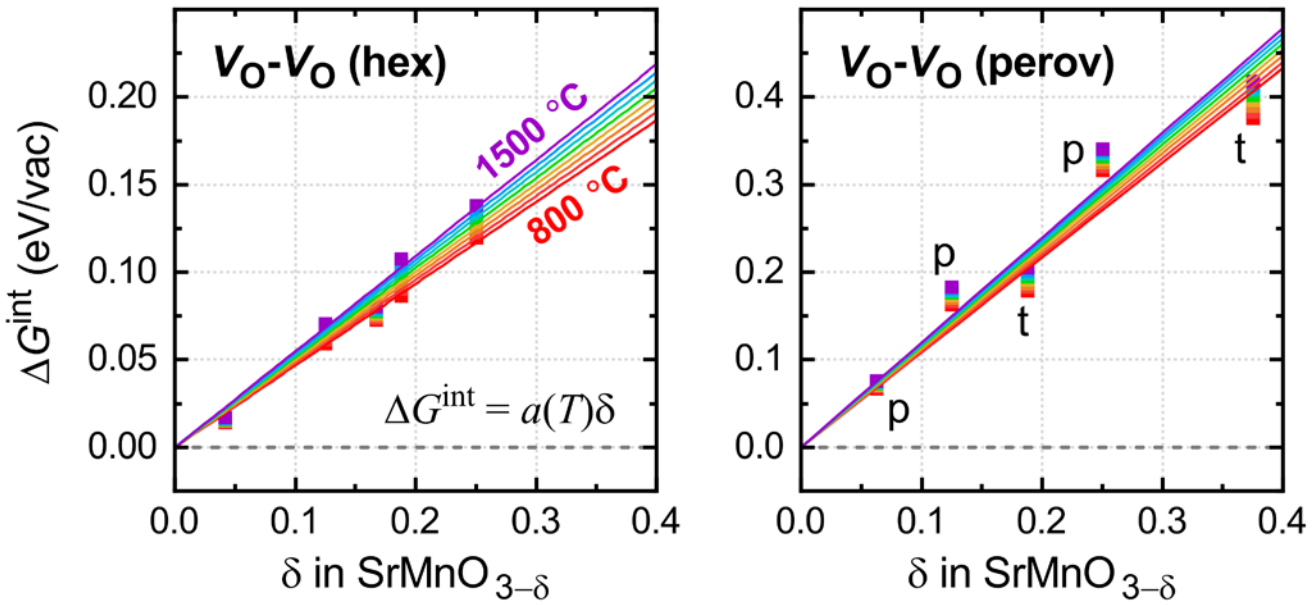

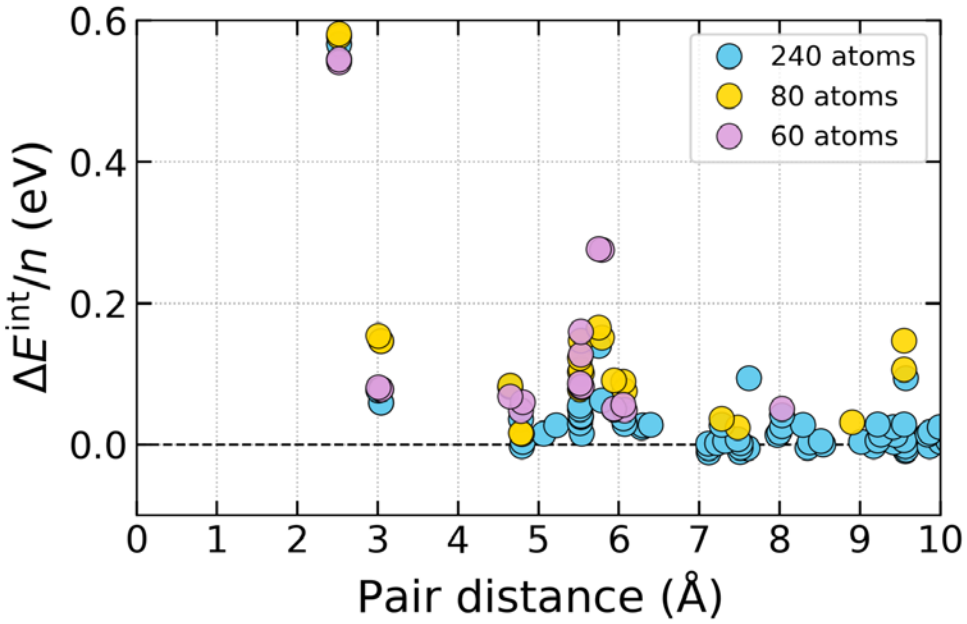

$SrMnO_3$ reduction

$$\Delta G^{\mathrm{tot}} = f_{\mathrm{d}}\left(x_{\mathrm{V}}\left(\Delta H_{\mathrm{D}} + \Delta G_{\mathrm{D}}^{\mathrm{int}}\right) + k_{\mathrm{B}}T\left(x_{\mathrm{V}}\ln(x_{\mathrm{V}}) + (1-x_{\mathrm{V}})\ln(1-x_{\mathrm{V}})\right)\right)$$

Interacting defect model

- δ moderately underestimated in both phases
- Very good description of *T*-dependence
- Slight adjustment of ΔH_D yields perfect agreement for all *T*

Hexagonal-perovskite phase transition

- ΔE_{poly} = 0.16 eV/fu in SCAN+U
  ΔG^{tot} = 0.13 eV/fu
- Possible additional contributions:
  - vibrational free energies and ZPE
  - polymorph energies beyond DFT

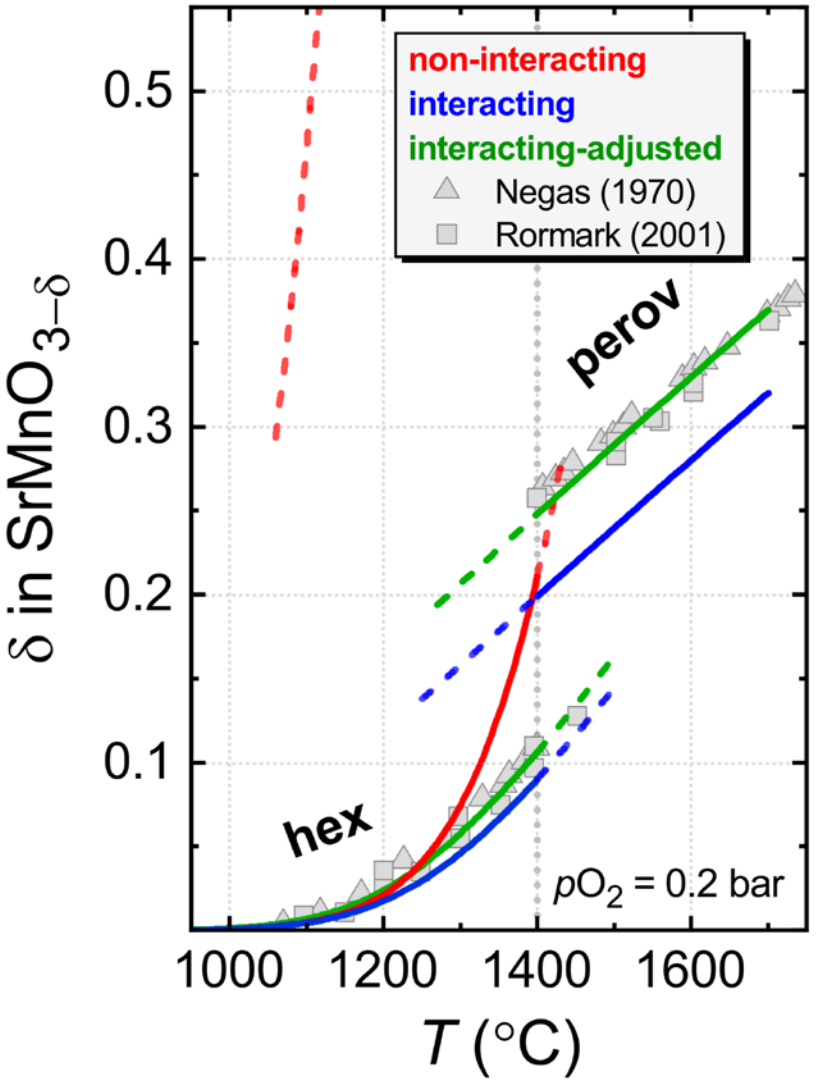

Ce alloying in $Sr_{1-x}Ce_xMnO_{3-\delta}$

Mixing enthalpy

- Positive ΔH_{mix} as expected for solid solution
- x = 1: $CeMnO_3$ is unstable wrt CeO_2+MnO
- Hexagonal-Perovskite transition at x = 0.1 (experimentally at x = 0.05)

O vacancy formation energies

- Strong x dependence
- Superposition of defect interactions:

$$\Delta G^{\mathrm{int}}(T) = (a_0 + a_1 T)\,\delta + (a_0' + a_1' T)\,x_{\mathrm{Ce}}$$

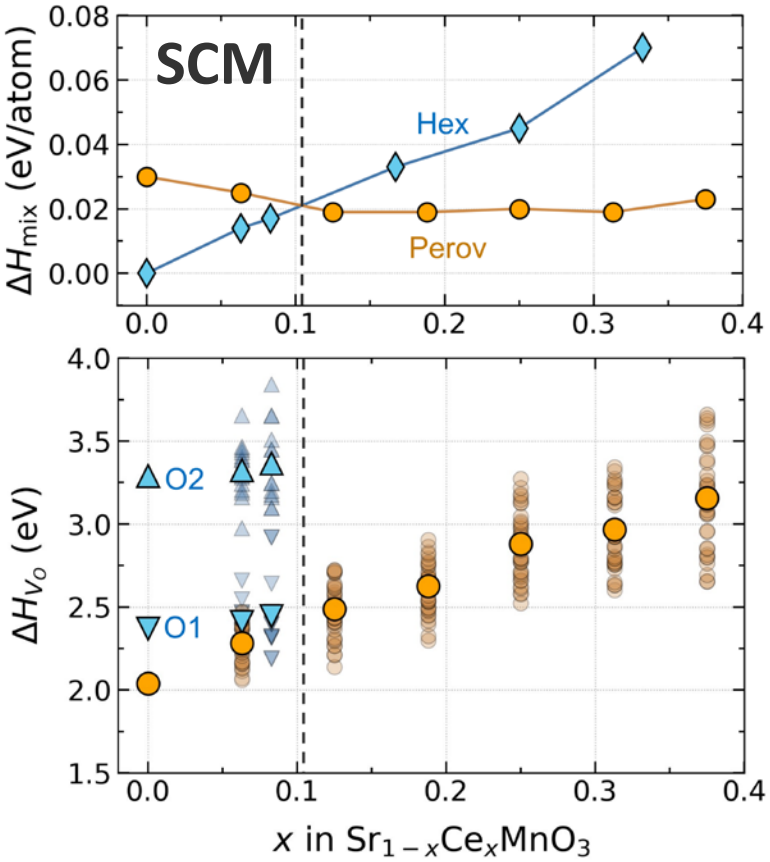

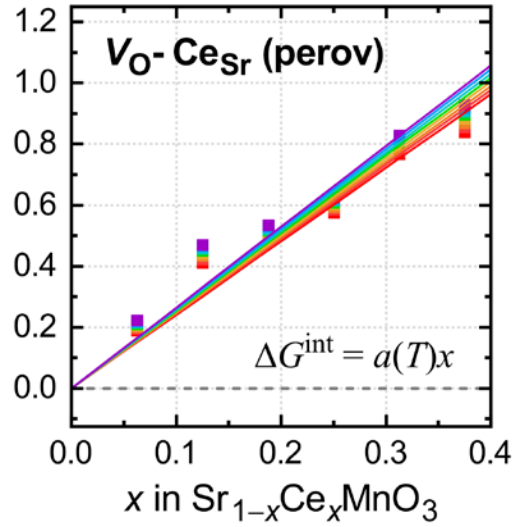

SCM reduction and H_2

- δ decreases with Ce fraction
- Almost quantitative agreement with experiment

Bergeson-Keller *et al*, Ene. Tech. (2022)

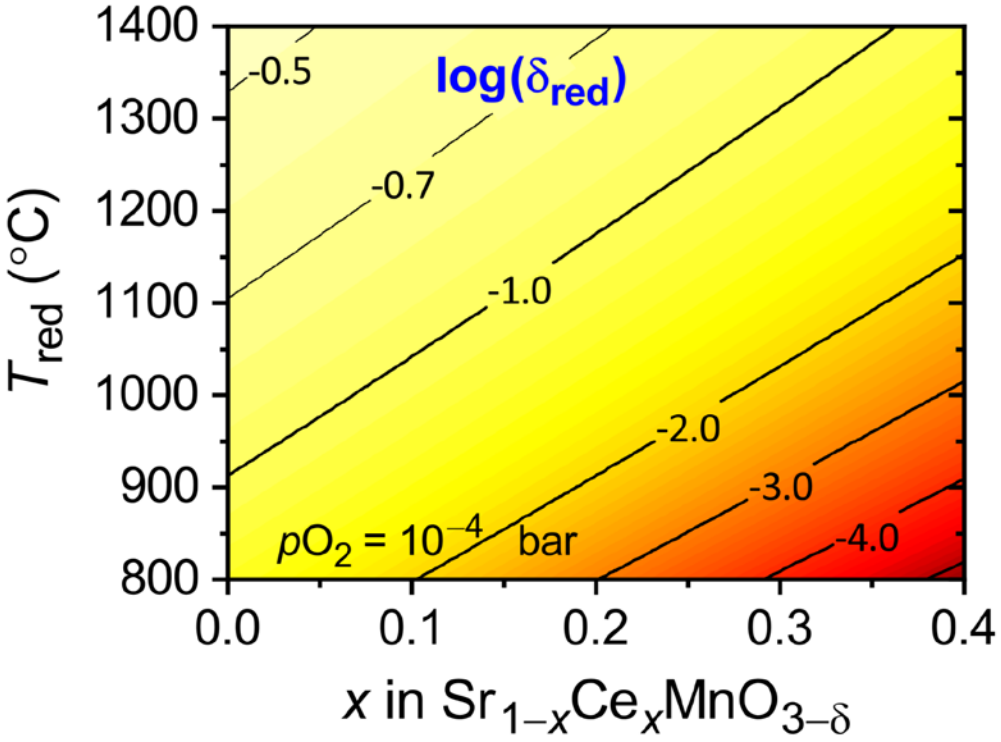

- Reduction: T = 1400 °C, $pO_2 = 10^{-4}$ atm
  Oxidation: T = 850 °C, pH_2O = 1 atm
- Ideal gas law: $H_2 + O_2 \leftrightarrow H_2O$
- Water splitting only under dilute H_2:H_2O
  $pH_2 < 10^{-2}$ atm
- Increasing pH_2 threshold with x_{Ce}

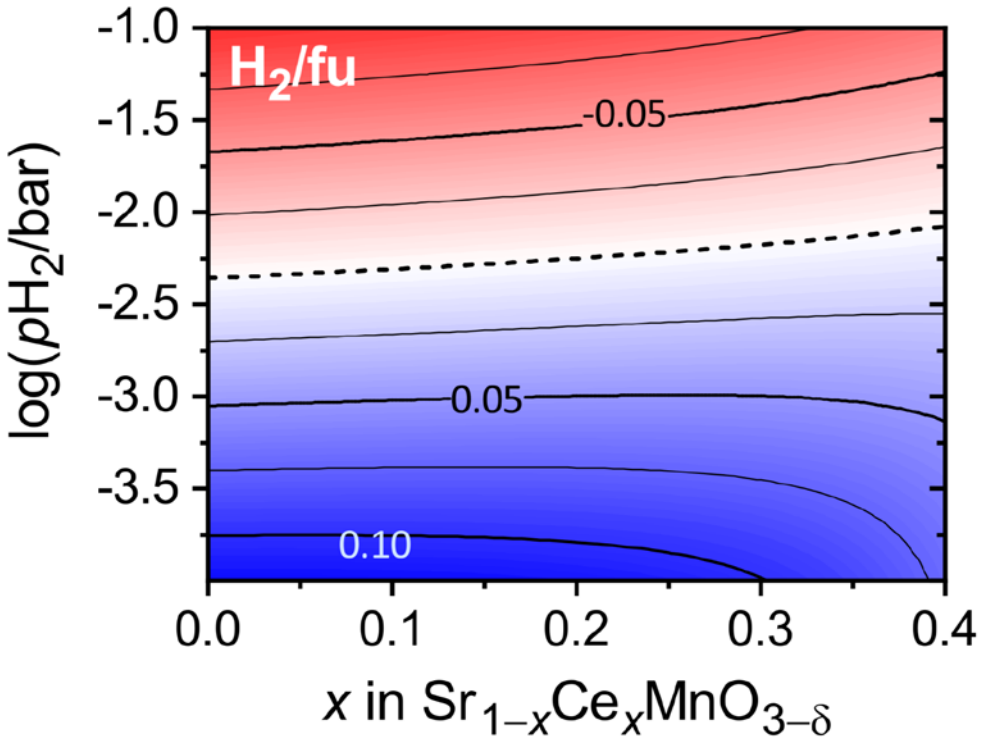

Interacting defects in STCH oxides: Conclusions

General model for repulsive defect interactions

- Sampling of defect pairs and triplets
- Free energy of defect interaction
- Parameterization $\Delta G^{\text{int}} = (a_0 + a_1 T)\,\delta$ and higher orders in T

A. Goyal, M.D. Sanders, R.P. O'Hayre, S. Lany, PRX Energy **3**, 013008 (2024)

STCH water splitting

- Very good agreement with expt. data (T-dependence)
- Work highlights STCH challenges in enthalpy-entropy tradeoff

Thank you

www.nrel.gov

NREL/PR-5K00-89067

This work was performed in part at the National Renewable Energy Laboratory, operated by Alliance for Sustainable Energy, LLC, for the U.S. Department of Energy (DOE) under Contract No. DE-AC36-08GO28308. Funding provided by the U.S. Department of Energy, Office of Energy Efficiency and Renewable Energy, Hydrogen and Fuel Cell Technologies Office and specifically the HydroGEN Advanced Water Splitting Materials Consortium, established as part of the Energy Materials Network under this same office. This research was performed under the project “Disorder in Topological Semimetals”, funded by the U.S. Department of Energy (DOE), Office of Science (SC), Basic Energy Sciences, Physical Behavior of Materials program. The views expressed in the article do not necessarily represent the views of the DOE or the U.S. Government. The U.S. Government retains and the publisher, by accepting the article for publication, acknowledges that the U.S. Government retains a nonexclusive, paid-up, irrevocable, worldwide license to publish or reproduce the published form of this work, or allow others to do so, for U.S. Government purposes.